Palaeomagnetic results from Upper Miocene and Pliocene rocks from the Internal Zone of the eastern Betic Cordilleras (southern Spain)

Manuel Calvo [a,c,*], Ramón Vegas [b], María Luisa Osete [c]

[a] *Géophysique et Tectonique, UMR CNRS 1760, Univ. Montpellier 2, 34095 Montpellier Cedex 5, France*
[b] *Dep. de Geodinámica, Universidad Complutense, 28040 Madrid, Spain*
[c] *Dep. de Física de la Tierra I, Universidad Complutense, 28040 Madrid, Spain*

Abstract

Palaeomagnetic and rock-magnetic studies were carried out on samples from thirteen volcanic and nine sedimentary sites of Late Miocene to Pliocene age from the Internal Zone of the eastern Betic Cordilleras. After comparing palaeomagnetic results with the expected Pliocene/Miocene direction, rotated and unrotated areas can be recognized, rotations being clockwise and counter-clockwise. Some rotations are of great magnitude. Unlike deformation in the External Betics, Late Miocene to Present block rotations in the Internal Betic Zone are non-systematic, and related to the movement of faults as local responses to the Late Miocene–Present regional stress field, due to the N140 convergence of Africa and the Iberian Peninsula.

Keywords: palaeomagnetism; rotation; Betic Cordillera; Neogene

1. Introduction

The Betic Cordilleras, which lie on the southern margin of Iberia, constitute one of the major elements of the western Mediterranean Alpine chain. Several palaeomagnetic investigations have been carried out there during the last 15 years, showing that block rotations about vertical axes have played an important role in deformation of the External Zones of this orogenic belt. In its central and western parts a consistent pattern of systematic clockwise 40–60° rotations has been found (Osete et al., 1988, 1989; Platzman, 1992; Platzman and Lowrie, 1992; Villalaín et al., 1994; Villalaín, 1995). All these studies have been performed on Mesozoic rocks, but a widespread Neogene remagnetization observed on Jurassic rocks in the western part of the External Betics (Villalaín et al., 1994) has put constraints on the age of the rotations, which have occurred after the remagnetization event, between Neogene and Present (Villalaín, 1995). Recent palaeomagnetic results from the Ronda peridotites, which lie in the Internal Zone of the western Betic Cordilleras yield a 46° clockwise rotation (Feinberg et al., 1996) which the authors consider to have taken place in a short span of time during post-metamorphic cooling of these units during Aquitanian to Burdigalian (Lower–Middle Miocene). Nevertheless, as (1) rotated palaeodeclinations are found in two stable an-

tipodal directions of magnetization and (2) despite relatively wide unblocking temperature spectra no trace of intermediate directions lying between unrotated and 46°-rotated palaeodeclinations are found in demagnetization plots, rotations probably occurred after cooling down of the peridotites.

Palaeomagnetic data in the eastern Betics have been sparse, although recently new results have been published. In the External Zones, a more heterogeneous behaviour than in the central and western Betics can be observed, with mainly clockwise, and sometimes very large rotations, and some regions which have experienced no rotation at all (Mazaud et al., 1986; Ogg et al., 1988; Osete et al., 1989; Allerton et al., 1993, 1994). In the Internal Zone, a palaeomagnetic study was carried out by Allerton et al. (1993) on a Permo–Triassic to Late Miocene sedimentary succession in Sierra Espuña, finding that 140° of a 200° clockwise rotation had taken place after earliest Miocene time and could have been finished in the Late Miocene, although it could not be assured that the unrotated Late Miocene direction found was not a recent overprint. Thus, the problem of determining the time of completion of rotations is still unsolved. On the other hand, a study on mainly volcanic rocks of Late Miocene age carried out by Calvo et al. (1994) in the Cabo de Gata region (Internal Betics), at the southeastern tip of Spain, has documented a behaviour different from the more systematic rotation pattern of the previously studied units in the External Betics, i.e. small clockwise and anticlockwise rotations of adjacent blocks.

The present palaeomagnetic study was started in order to obtain more information about occurrence and geographical distribution of possible recent palaeomagnetic rotations in southeastern Spain, specifically in the Internal Betic Zone, in order to study the tectonic setting in this area during Late Miocene to Recent deformation.

2. Geological setting

The present study has been carried out on samples belonging to Neogene intramontane basins and their associated volcanism in the eastern Betic region, in the southeastern part of the Iberian Peninsula. Neogene intramontane basins can be found throughout all the Betic region. Their formation is related to an extensional episode which started in the late Aquitanian/Burdigalian (Comas et al., 1992) and finished in the middle or late Tortonian. In southeastern Spain two types evolved simultaneously: narrow and elongated strongly subsiding basins and grabens of smaller development (Montenat et al., 1987). In close relation with these basins a set of long NE–SW- to N–S-trending left-lateral strike-slip faults accompanied by a conjugate set of shorter NW–SE right-lateral strike-slip faults can be recognized in this region (Fig. 1). These Pliocene/Quaternary faults postdate the extensional episode responsible for basin formation (e.g., Vegas, 1992), although some authors consider the fault system to be related to basin genesis (Montenat et al., 1987; de Larouziere et al., 1988).

Neogene volcanism in southeastern Spain is also related to fault activity and basin formation. The volcanic area in this region stretches more than 100 km northwards from the Mediterranean coast to the interior. It can be also followed southwards into the Alborán Sea. From a petrological point of view, four types of volcanic rocks can be distinguished (Araña and Vegas, 1974; López Ruiz and Rodríguez Badiola, 1980; Bellon et al., 1983): (a) calc-alkaline volcanics, with K/Ar ages between 8 and 12 to 15 m.y.; (b) potassic calc-alkaline and shoshonitic volcanics, with K/Ar ages between 6.6 and 8.3 m.y.; (c) lamproitic volcanic rocks with K/Ar ages between 5.7 and 8.6 m.y.; (d) basaltic alkaline volcanics, with K/Ar ages of 2.7 and 2.8 m.y. (K/Ar ages from Bellon et al., 1981a,b, 1983; Nobel et al., 1981; Di Battistini et al., 1987).

3. Sampling and laboratory methods

For the present study, thirteen volcanic and nine sedimentary sites with ages ranging between Late Miocene (Tortonian) to Plio/Quaternary were sampled. From the thirteen volcanic sites, two belong to potassic calc-alkaline volcanism, seven to lamproitic volcanism and four to basaltic-alkaline volcanism (Table 1, Fig. 1). Calc-alkaline volcanism was sampled for another study, and results are reported elsewhere (Calvo et al., 1994). Each sampled volcanic site represents a single volcanic flow, dome or dyke. The range of vertical sampling in sedimentary sites varied from 2 to 50 m. From each site six to fifteen

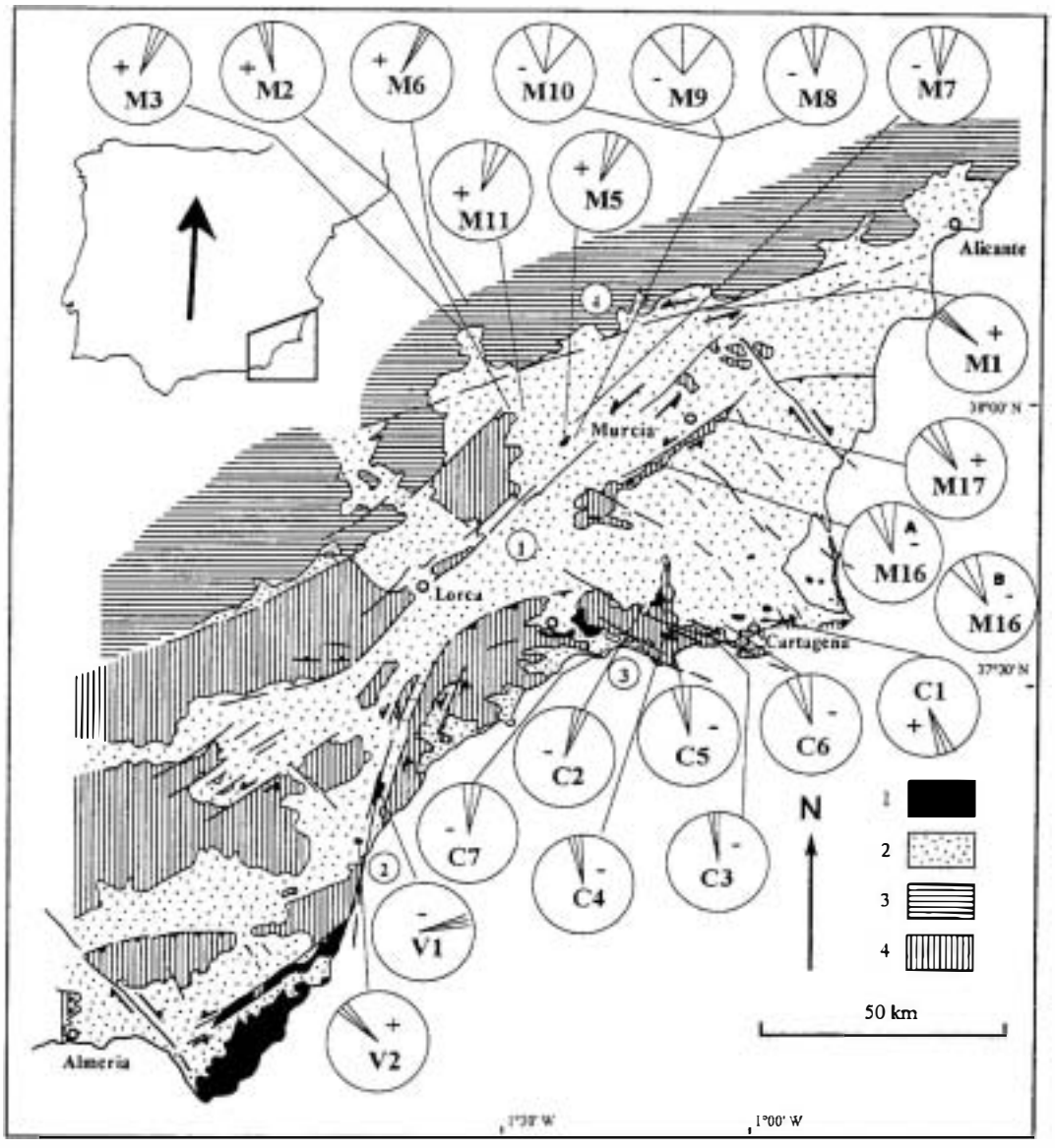

Fig. 1. Schematic geological map from southeastern Spain and palaeomagnetic results: *1* = volcanics; *2* = Neogene basins; *3* = External Betics; *4* = Internal Betics. Numbers in circles: *1* = Lorca fault zone; *2* = Palomares fault zone; *3* = Cartagena fault zone; *4* = Crevillente fault zone. Circles show palaeodeclinations with confidence limits (Demarest, 1983) and polarity (+: normal, −: reversed). The thick arrow at the upper-left corner shows the expected Pliocene–Miocene direction (Besse and Courtillot, 1991; Bógalo et al., 1994).

(in most cases eleven to thirteen) cores were taken with a portable drill, and one to five specimens were cut from each core. Cores were oriented by means of a magnetic compass as well as a sun compass in volcanic sites. Local structural study, general bedding attitude of sampling areas and interbedded sediments in one case, were used for bedding correction of volcanic formations, shallow dips (or no dip at all) being obtained in most cases. In several sites, where dip values lower than 5° and unclear strike values

Table 1
Palaeomagnetic results

Site	Unit	Age	N	GC Dec	GC Inc	SC Dec	SC Inc	k	α_{95}	Rot	BC
C1	CAP	*7.2 m.y.	10	155.9	14.9	157.9	34.6	48.8	7.0	155.0	235,20 N
V1	CAP	*8.2/7.6 m.y.	9	242.5	−42.3	256.6	−47.6	97.4	5.2	73.7	90,15 S
M1	LAM	*6.1 m.y.	11	310.6	43.2	310.2	48.2	238.7	3.0	−52.7	45,5 S
M2	LAM	5.7–8.6 m.y.	9	349.5	65.6			298.1	3.0	−16.3	dip=●
M3	LAM	5.7–8.6 m.y.	13	22.9	58.3			83.4	4.6	20.0	dip=●
M4	LAM	5.7–8.6 m.y.	6	326.3	17.3			148.0	5.5		dip<5
M5	LAM	*6.2–7 m.y.	10	21.5	61.1			51.0	6.8	18.6	dip<5
M6	LAM	5.7–8.6 m.y.	9	28.0	32.1			308.9	2.9	25.1	dip<5
V2	LAM	*Messinian [b]	12	314.1	67.8			174.9	3.3	−48.8	dip=●
C2	BAV	*2.42–2.58 m.y. [a]	9	198.2	−48.5			111.5	4.9	15.3	dip=●
C3	BAV	2.42–2.58 m.y. [a]	12	174.0	−45.0			72.2	5.1	−8.9	dip=●
C4	BAV	*2.42–2.58 m.y. [a]	12	169.9	−64.4			111.9	4.1	−13.0	dip=●
C5	BAV	2.42–2.58 m.y. [a]	5 (0/5)	168.3	−48.2	170.5	−47.0	171.4	8.6	−12.4	300,3 N
M7	SED	Messinian	15 (1/14)	177.7	−39.7	185.0	−46.0	10.8	12.6	2.1	40,10 S
M8	SED	Messinian	7	271.7	−58.8	176.9	−56.5	40.5	9.6	−6	226,50 N
M9	SED	Messinian	8 (2/6)	270.9	−58.0	178.6	−56.3	6.9	24.1	−4.3	226,50 N
M10	SED	Messinian	5 (3/2)	253.8	−52.8	187.2	−46.7	11.2	25.4	4.3	226,50 N
M11	SED	Plio–Quat.	9 (8/1)	19.2	50.4			26.4	10.3	16.3	dip=●
M16 [A]	SED	Messinian	12 (0/12)	173.1	−38.2	165.6	−57.1	23.9	9.8	−17.3	99,20 S
M16 [B]	SED	Messinian	8	339.9	30.7	330.8	47.5	35	9.5	−32.1	99,20 S
M17	SED	Serrav.–Tort.	9	326.4	10.6	333.8	46.5	30.7	9.7	−29.1	40,38 N
C6	SED	Messinian	10 (0/10)	164.6	−41.6	164.6	−33.6	13.2	15.2	−18.3	255,8 N
C7	SED	Tortonian	19 (0/19)	178.9	−49.7	184.5	−39.1	29.3	6.6	7.4	300,12 N

Site: site number (in site M16, A: component A; B: component B, see text). Unit: CAP is calk-alkaline and potassic volcanism; LAM is lamproitic volcanism; BAV is basaltic alkaline volcanism; SED is sedimentary rocks. Age: age of sites (see text); an asterisk shows volcanic sites where an age determination has been carried out. N is number of cores. In brackets: number of directly determined directions and number of planes. GC: geographic coordinates (without tectonic correction). SC: stratigraphic coordinates (with tectonic correction). In several sites with dip <5° and unclear strike, no tectonic correction was applied. Dec: declination. Inc: inclination. k: precision parameter. α_{95}: radius of 95% confidence circle. Rot: rotation of palaeodeclination with respect to expected direction (see text). BC: bedding correction (strike and dip, in degrees; dip direction: N is north; S is south).

[a] Sites where radiometric ages have been delimited more precisely with palaeomagnetic results from this study (see text).

[b] Völk (1966).

were observed, no tectonic correction was applied (Table 1).

Remanent magnetization of volcanic sites was measured with a Molspin spinner magnetometer in the palaeomagnetic laboratory of the Complutense University of Madrid, while sedimentary samples were measured with a CTF cryogenic magnetometer in the University of Montpellier. These latter measurements were recorded after stabilization of remanence in the cryogenic magnetometer, which was made possible with an application code which permitted plotting of magnetization changes in real time (Levêque, 1992). For each site, one or two pilot samples were chosen for stepwise thermal demagnetization up to 600–700°C and another one was chosen for stepwise AF cleaning, with peak-field values of 100 to 200 mT. According to the results of the preliminary experiments, all other samples were subjected to thermal or AF demagnetization, choosing the suitable demagnetization values, although normally only a small number of samples from sedimentary sites was subjected to the latter treatment. Nevertheless, in several cases sedimentary samples were subjected to a combined treatment, so that after an initial AF treatment up to 20 mT a thermal demagnetization was applied. During thermal demagnetization, initial susceptibility at room temperature was measured after each step, to check if chemical and/or mineralogical changes had taken place in magnetic minerals during heating. The usual num-

Table 2
Rock-magnetic results

Site	T_C (°C)	SIRM (A m^{-1})	I_{RS}/I_S	H_{CR}/H_C	MDF (mT)	INT (mA m^{-1})	MIC	AMS-P
C1	495	12.7	0.09	3.3	19.5	273	Mt, (Mgh)	1.0893
V1	490	0.0735	0.005–0.01	–	37.0	1.8	Mt, Frt, Ilm	1.0514
M1	460	0.357	<0.005	–	43.5	19.0	Mt, (Mgh), (Ilm)	1.0109
M2	–	6.2	0.17	–	60.5	61.2	Mt, Ht, (Ilm)	1.0221
M3	425?	4.06	0.08	–	60.5	138	Mt, (Ilm)	1.0190
M4	570	13.6	0.08	3.0	–	277	–	1.0208
M5	580	7.2	0.09	3.3	>63.5	682	Mt, Tht, Fes, Ilm	1.0159
M6	–	7.73	<0.03	–	19.0	18	Mt, Mgh, Tht, Frt	1.0072
V2	520	1.78	0.005–0.01	–	>72.5	121	Mt, Tht	1.0147
C2	535	329	0.15	2.7	10.0	744	Mt, Mgh, Ilm	1.0064
C3	–	–	–	–	53.0	3309	–	1.0232
C4	–	–	–	–	24.0	5325	–	1.0168
C5	–	–	–	–	4.7	30125	–	1.0212

Site: site number. T_C: Curie temperature. SIRM: intensity of remanent isothermal saturation magnetization. I_{RS}/I_S: remanent saturation to saturation magnetization ratio. H_{CR}/H_C: coercivity of remanence to coercivity ratio. MDF: median destructive field. INT: intensity of remanence. MIC is ore microscopy: Mt, magnetite; Mgh, maghemite; Tht, titano-hematite; Frt, ferri-rutile; Ilm, exsolved ilmenite lamellae; Ht, hematite; Fes, iron-sulfide. AMS-P is anisotropy factor.

ber of demagnetization steps was between 12 and 15, but this number was enhanced (or reduced) to a maximum (or minimum) value of 22 (or 6), depending on the complexity of palaeomagnetic behaviour of the studied samples. Directions of magnetization components were calculated by means of principal component analysis (Kirschvink, 1980).

Palaeomagnetic site means for volcanic sites were calculated using Fisher statistics (Fisher, 1953). Mean directions in most sedimentary sites and volcanic site C5 were calculated combining directly determined directions and remagnetization circles (McFadden and McElhinny, 1988).

In order to identify the magnetic carriers responsible for remanent magnetization and to obtain information about their palaeomagnetic stability, several rock-magnetic experiments were carried out (Table 2, Fig. 4). Most of these experiments were performed at the palaeomagnetic laboratory of the Ludwig-Maximilian University of Munich. These experiments included: (a) measurement of induced magnetization versus temperature by means of a Curie balance and determination of Curie temperatures; (b) measurement of hysteresis parameters (coercivity H_C, coercivity of remanence H_{CR}, remanent saturation I_{RS} and saturation magnetization I_S); (c) measurement of isothermal remanent magnetization (IRM) acquisition curves; and (d) thermal demagnetization of two perpendicular IRM created in a strong (0.9 or 1.6 T) and a weak (0.1 T) field (Lowrie and Heller, 1982). In addition, measurements of anisotropy of magnetic susceptibility (AMS) and ore-microscopic studies were carried out. Sedimentary rocks were only subjected to IRM acquisition and demagnetization experiments.

4. Results

4.1. Potassic calk-alkaline rocks

Palaeomagnetic behaviour during demagnetization of both studied sites (C1 ad V1) is simple, as only one palaeomagnetic component together with a small viscous component is found. C1 shows a narrow unblocking temperature spectrum, samples being demagnetized mainly between the 550°C and the 600°C steps. Characteristic remanent magnetization (ChRM) thus seems to be carried by magnetite or low-Ti titanomagnetite. The observed Curie temperature is, however, lower than that of pure magnetite (Table 2). Curie temperature determination for both sites was, nevertheless, somewhat difficult, as the decrease in intensity of magnetization in the measured thermomagnetic curves (one per site) took place

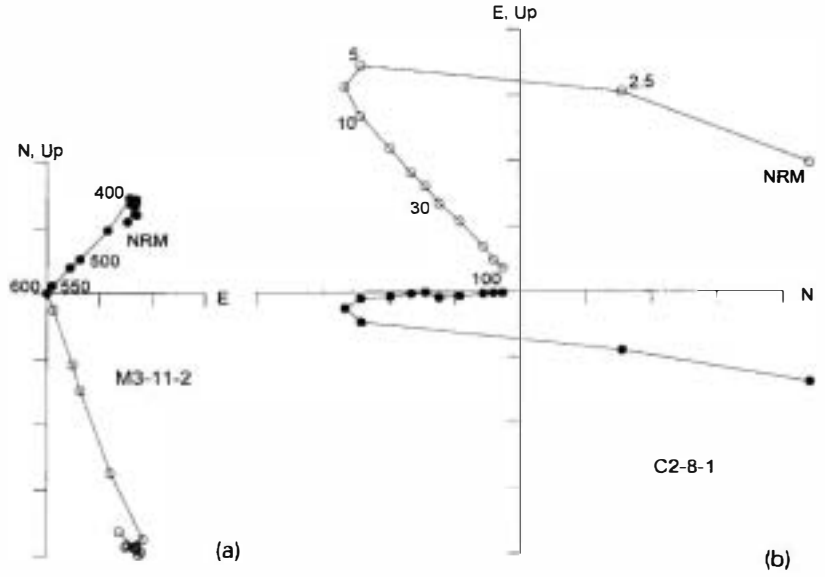

Fig. 2. Demagnetization of volcanic samples: dots are for the horizontal projection and circles for the vertical projection. (a) Thermal demagnetization of sample M3-11-2 (lamproitic volcanism). Demagnetization steps in °C. (b) Alternating field demagnetization of sample C2-8-1 (basaltic alkaline volcanism). Demagnetization steps in mT.

gradually, in a relatively broad temperature interval. ChRM in V1 also seems to be carried by low-Ti titanomagnetite and by another high-coercivity mineral with low unblocking temperature — probably titanohematite — as shown by demagnetization of IRM and NRM. The presence of these kinds of titanohematites would be also in agreement with the low NRM and IRM intensities observed in V1 (Table 2). ChRM shows strongly rotated palaeodeclinations in both cases (Table 1).

4.2. Lamproitic rocks

Six sites (M1, M2, M3, M4, M6 and V2) show a simple palaeomagnetic behaviour, as only one component can be recognized during demagnetization (Fig. 2a). In M4 remanence is carried by magnetite, as shown by unblocking temperatures during demagnetization and Curie temperature (Table 2). Unblocking temperatures of NRM and IRM demagnetization of the other five sites show the presence of low Ti-titanomagnetite or magnetite, but high-coercivity phases are also present as carriers of remanence. Curie temperatures are difficult or impossible to determine, as magnetization intensities are low in most cases. Values obtained lie between 425 and 520°C. Often AF demagnetization cannot be completed and MDF values are generally high (Table 2). Saturation IRM (SIRM) values are low. Ore microscopy shows the presence of magnetite and in some cases also maghemite and titanohematite. This latter mineral could be responsible for the high-coercivity component. In samples of site M5 two components can be recognized. Remanence is carried by magnetite and also by titanohematite. In all sites magnetic minerals show a low degree of alteration. Magnetic polarities of ChRM are normal, and in most cases declinations deviate moderately from the north (Table 1). Inclination of M4 shows a shallow value of 17.3°. As its dip is smaller than 5°, anisotropy of magnetic susceptibility is weak and NRM consists of only one palaeomagnetic component, this anomalous inclination could be explained as being due to a feature of the geomagnetic field during remanence formation, and for this reason the results of this site have not been considered.

4.3. Basaltic alkaline rocks

Four sites (C2, C3, C4 and C5) were studied. Rock-magnetic data were available only for samples from C2, but all four sites belong to the same kind

of volcanism, have similar age and are located not far away from each other (Fig. 1). Microscopic studies show the presence of magnetite and exsolved ilmenite lamellae in C2, thus indicating the occurrence of high-temperature oxidation. Demagnetization of NRM shows that C3 has only one palaeomagnetic component, which is of reversed polarity, remanence being carried by magnetite or low-Ti titanomagnetite. All other three sites show a two-component behaviour. ChRM is of reversed polarity, probably being carried by low-Ti titanomagnetite. In sites C2 and C4 ChRM can be isolated (Fig. 2b), but in most cases not the first component, which seems to have a present-day field direction. In C5, both components overlap during the whole demagnetization procedure, and remagnetization circles had to be used for ChRM determination. Palaeodirections are directed southwards and are of reversed polarity, thus being unrotated (Table 1). K–Ar ages of these sites lie between 2.69 ± 0.27 and 2.80 ± 0.23 m.y. (Bellon et al., 1983), their ChRM thus belonging to normal polarity chron C2An.1n (Cande and Kent, 1995), a fact which apparently contradicts palaeomagnetic results. If confidence limits of the radiometric ages are, however, taken into account, these units can be dated in a more precise way, being placed in the upper part of chron C2r.2r, with an age lying between 2.42 and 2.58 m.y.

4.4. Sedimentary rocks

Sites M7, M8, M9 and M10 (sandstones and marly limestones) are of Messinian age. They are located close to the Lorca fault (Fig. 1). Palaeomagnetic analysis yields two main components: a secondary normal-polarity component of northerly direction and a primary reversed-polarity component with a southerly direction after bedding correction (Fig. 3). The latter component is carried by magnetite, which is also shown by IRM acquisition and demagnetization experiments (Fig. 4). In a few samples of M8 and M9 a third component, carried by hematite and of reversed polarity, can be recognized (Fig. 3). It has a southerly direction before and an anomalously low inclination after bedding correction, and is therefore a secondary component. Isolation of ChRM in sites M7, M9 and M10 is difficult, as unblocking temperature and coercivity spectra of

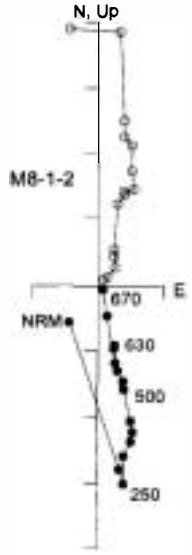

Fig. 3. Thermal demagnetization of sedimentary sample M8-1-2. Data are plotted in stratigraphic coordinates (after tectonic correction). Dots are for the horizontal projection and circles for the vertical projection. Demagnetization steps in °C.

both main components are often similar, with unblocking temperatures being somewhat higher for the primary component. Mineralogical changes beginning at temperatures over 400 or 500°C in M7 and M10 often hinder a straight interpretation of demagnetization plots. For this reason, mean ChRM directions for sites M7, M9 and M10 had to be calculated combining directly determined directions and remagnetization circles, and the within-site scatter in these sites is high (Fig. 5).

In site M11 (Plio–Quaternary travertines), after demagnetizing a viscous component, only a northwards directed normal-polarity direction —probably carried by magnetite— can be found.

South of the city of Murcia two sites were sampled: Messinian calcarenites at Sierra del Puerto (M16) and Serravalian to early Tortonian sandstones at Sierra de Columbares (M17) (Fig. 1). In the latter, ChRM has a northwestward pointing normal-polarity direction after bedding correction (Fig. 6a). This component is probably carried by hematite, as demagnetization experiments show that a significant amount of magnetization is left above 575°C, and the IRM acquisition curve (Fig. 7) clearly shows the presence of a high-coercivity phase. Mineralogical

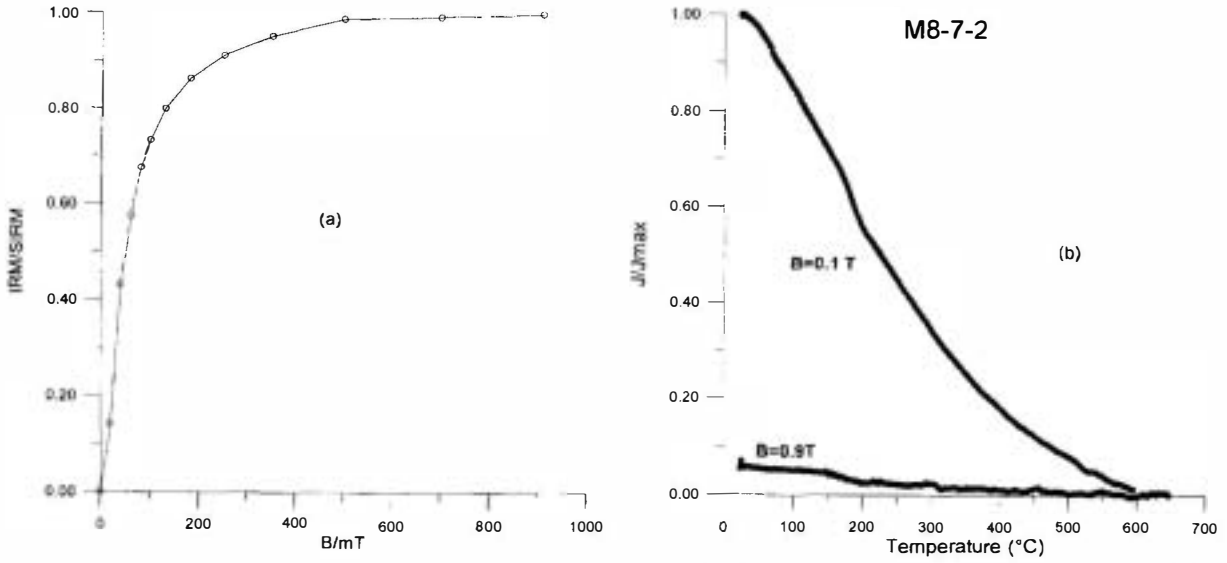

Fig. 4. IRM acquisition and demagnetization curves for sedimentary sample M8-7-2. (a) Acquisition curve. *IRM/SIRM* = normalized intensity of remanence. Saturation remanence = 5.91×10^{-4} Am^2/kg. (b) Continuous thermal demagnetization of two perpendicular components of remanence with a vibrating-sample thermomagnetometer. One component was acquired in a field of $B = 0.9$ T and the other one in a subsequently applied field of $B = 0.1$ T. *J/Jmax* = normalized intensity of magnetization.

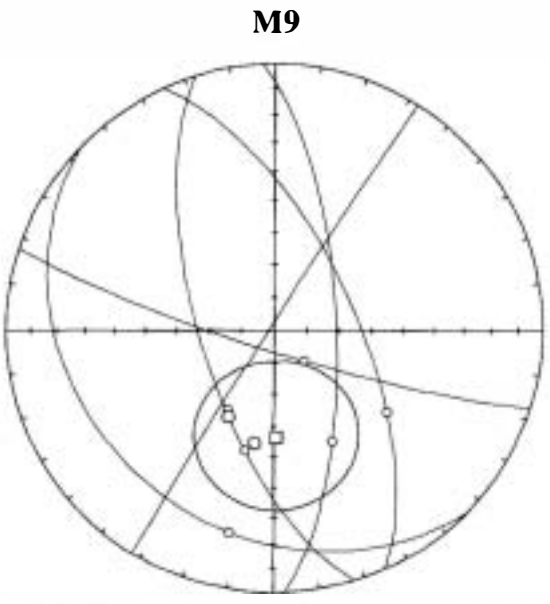

Fig. 5. Mean direction and α_{95} for site M9 (after McFadden and McElhinny, 1988). Data are plotted in stratigraphic coordinates (after tectonic correction). Small dots: directions determined from great circles. Big dots: directly determined directions. Square: mean direction ($D = 178.6$, $I = -56.3$, $N = 8$, $k = 6.9$, $\alpha_{95} = 24.1$). Half great circles with negative inclinations are shown.

changes at high temperatures (Fig. 6b) often hamper interpretation of the last demagnetization steps. Together with ChRM, often a secondary component of low unblocking temperatures with a present-day field direction can be recognized. Mean ChRM in these sites was calculated combining directly determined directions and remagnetization circles (Fig. 8). In site M16, a reversed polarity component (component A) and a normal-polarity and northwesterly directed component (component B) are found (Fig. 6c). They are in most cases partially overlapped. Most of the samples are completely demagnetized at temperatures around 350–400°C. Often the last steps are difficult to interpret due to magneto-mineralogical changes. In most cases, isolation of primary component A, which could be carried by pyrrhotite, is not possible. Nevertheless, remagnetization circles allow to determine ChRM, a southerly reversed-polarity direction being obtained after applying bedding correction. Despite its low unblocking temperatures ($T_{DB} < 250$ to 350°C), also the normal polarity component could be of primary origin, as inclination shows a value close to the expected Pliocene/Miocene direction ($D = 2.9°$, $I = 49.3°$, calculated from poles from Besse and Courtillot,

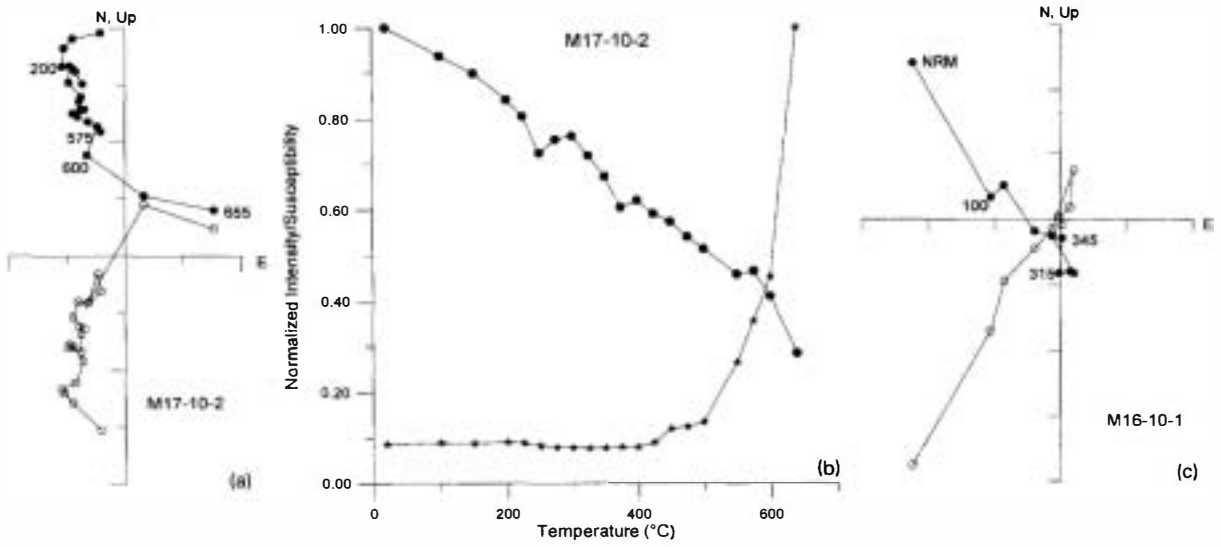

Fig. 6. Thermal demagnetization of sedimentary samples. Data are plotted in stratigraphic coordinates (after tectonic correction). Dots are for the horizontal projection and circles for the vertical projection. Demagnetization steps in °C. (a) Orthogonal vector plots for thermal demagnetization of sample M17-10-2. (b) Normalized intensity (J/J_{max}) and susceptibility at room temperature (K/K_{max}) during thermal demagnetization of sample M17-10-2. (c) Orthogonal vector plots for thermal demagnetization of sample M16-10-1.

1991 and Bógalo et al., 1994) after applying bedding correction ($D = 339.9°$, $I = 30.7°$ before and $D = 330.8°$, $I = 47.5°$ after bedding correction). Directions of both components are included in Table 1 and Fig. 1.

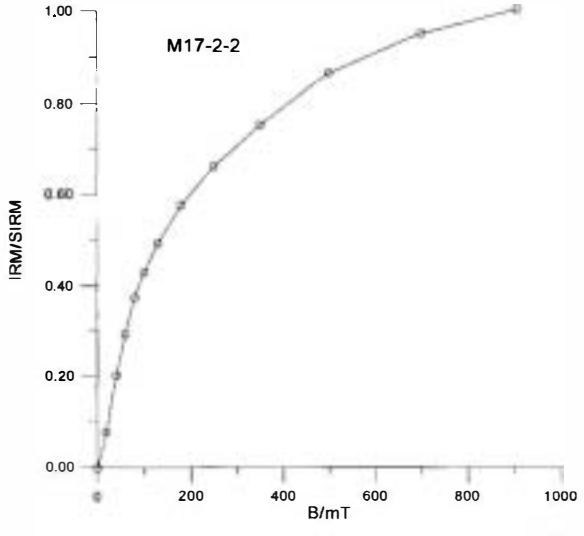

Fig. 7. IRM acquisition curve for sedimentary sample M17-2-2: *IRM/SIRM* = normalized intensity of remanence. Saturation remanence = 2.2×10^{-4} Am^2/kg.

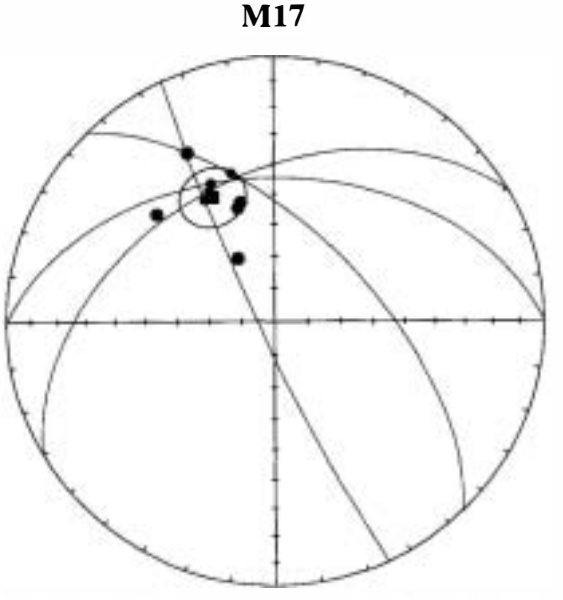

Fig. 8. Mean direction and α_{95} for site M17 (after McFadden and McElhinny, 1988). Data are plotted in stratigraphic coordinates (after tectonic correction). Small dots: directions determined from great circles. Big dots: directly determined directions. Square: mean direction ($D = 333.8$, $I = 46.5$, $N = 9$, $k = 30.7$, $\alpha_{95} = 9.7$). Half great circles with positive inclinations are shown.

At the southern edge of the Murcia province, two sites were sampled: Messinian sandstones (C6) and marly limestones of Tortonian age (C7) (Fig. 1). In both cases, two overlapping components of differing polarity can be found during demagnetization. Magneto-mineralogical changes at temperatures over 400°C do not allow to isolate ChRM, but also in this case remagnetization circles can be used to determine ChRM, which shows an unrotated reversed-polarity direction. A combined treatment of AF-demagnetization up to 15 to 20 mT followed by thermal demagnetization, yields the best results.

5. Discussion and conclusions

We consider ChRM as being probably of primary origin since: (a) normal and reversed ChRM directions were detected; (b) in many sites, a part of NRM carried by minerals of low unblocking temperature and coercivity shows a present-day field direction, which is different from the ChRM found in the same rocks, which is carried by stable minerals; (c) volcanic rocks show only a low-degree of alteration; (d) ChRM in several sedimentary sites shows reasonable inclination values only after bedding correction (e.g. M17).

After comparing palaeomagnetic results obtained for each site with the expected Pliocene/Miocene direction ($D = 2.9°$, $I = 49.3°$), it can be recognized that palaeodeclinations deviate sometimes from the expected direction of declination (Figs. 1 and 9, Table 1). Nevertheless, in most cases, this deviation is small, although some sites, which will be discussed in more detail later, show strong deviations of their declination. The mean inclination ($I_m = 53°$) calculated for all sites except M4 and the most rotated two, fits the expected value (Fig. 9).

In volcanic sites, anisotropy of magnetic susceptibility (AMS), which could be a source of anomalous palaeomagnetic directions, is generally weak (Table 2), but in two sites — C1 and V1 — higher values of AMS are observed (anisotropy factor $P = 1.09$ for C1 and $P = 1.05$ for V1). In most non-metamorphosed igneous rocks with anisotropy factors not exceeding ~1.2 the deviation of a thermal remanent magnetization (TRM) from the ambient field should be small (<5°), (Collinson, 1983), and therefore AMS cannot explain the strong rotations of palaeodeclination observed in some cases, even not those of sites C1 and V1. Another fact that should be taken into account in volcanic sites as a source of perturbation of the expected palaeomagnetic direction is secular variation. Some sites, however, show significant rotations which seem to exceed the range of those variations. The probability that those rotations are all due to geomagnetic excursions has been considered neglectable, in particular because inclinations do not deviate from the expected value over the range of secular variation. As it has already been mentioned, in site M4 a geomagnetic excursion during remanence formation could be nevertheless responsible for its anomalous palaeomagnetic direction (Table 1).

As already mentioned, most of the 22 studied sites show only a weak deviation of the palaeodeclination from the expected direction. Since in volcanic sites palaeosecular variation could be responsible of at least a part of this deviation, we have considered rotations in most cases not to be significant. Nevertheless, volcanic site M1, located close to the Crevillente fault (sinistral in Late Miocene–Pliocene), shows a strong counter-clockwise rotation, which confirms a movement between 6.1 m.y. to present (Table 1) in this fault. Also volcanic sites V1 and V2, which are located at both sides of the Palomares fault, show significant rotations. Both sites are, however, rotated in opposite senses. This behaviour can be explained in two ways: a 123° clockwise rotation followed by a 49° counterclockwise rotation: or as V1 is older than V2. a succession of counter-clockwise rotations: 238° between 8.2/7.6 m.y. and Messinian (Table 1), and 49° afterwards. Volcanic site C1 (late Tortonian) also displays a strongly (clockwise?) rotated palaeodeclination of 155°, too strong to be explained as due only to secular variation and AMS. Palaeodeclinations in most sedimentary sites do not deviate significantly from the expected direction. Calculated rotation values are relatively small (Table 1), and even in sites M11, M16 (component A) and C6, where they exceed 15°, they cannot be considered significant, as their confidence limits (Fig. 1) are of the same order of magnitude. Nevertheless, sedimentary site M17 (Serravalian–lower Tortonian) and component B in nearby lying site M16 (Messinian) display clearly counter-clockwise rotated palaeodeclinations, prob-

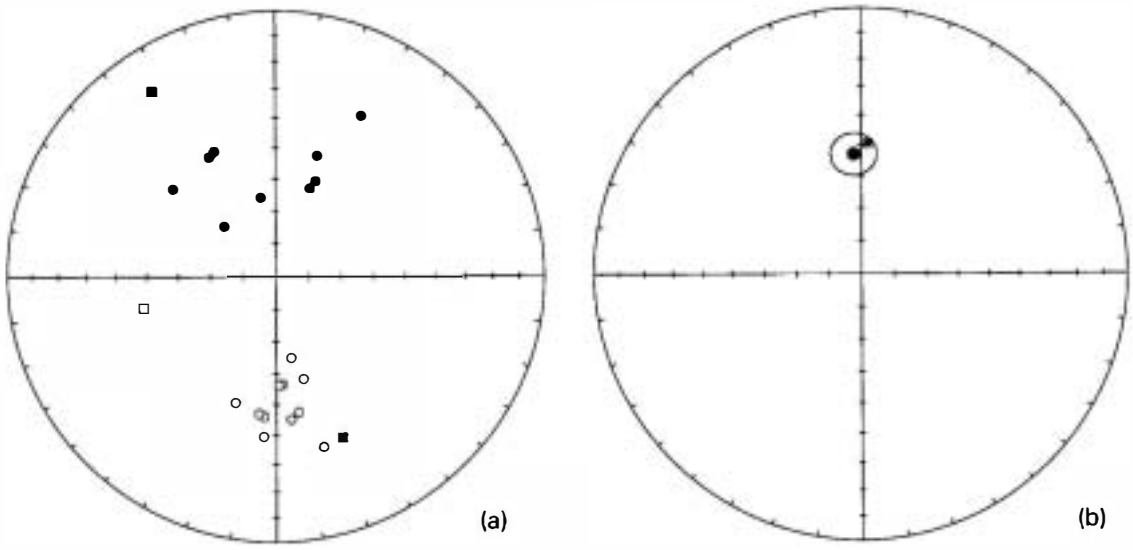

Fig. 9. Stereograms with mean directions of all sites. Data are plotted in stratigraphic coordinates (after tectonic correction) where needed (see Table 1). (a) Palaeomagnetic mean directions of all sites. Dots: sites considered for calculating the mean direction. Squares: sites not considered for calculating the mean direction (see text). Full symbols: normal polarity directions. Open symbols: reversed polarity directions. (b) Dot: calculated mean direction (D = 356.3, I = 52.8, k = 24.2, α_{95} = 6.8, N = 20). α_{95} is also shown. Asterisk represents expected direction (after Besse and Courtillot, 1991; Bógalo et al., 1994).

ably related to the movements of a closely located left-lateral fault (Fig. 1).

Some areas clearly appear to be unrotated. In the southern edge of the Murcia province, sites C2, C3, C4, C5, C6 and C7 (Pliocene to Tortonian age) yield a mean palaeomagnetic direction (D = 356.9°, I = 46.8°, α_{95} = 11.3) equal to the expected one. Also sites M7, M8, M9 and M10 (Messinian age), located not far away from the Lorca fault zone, show no palaeomagnetic rotation. Although within-site scatter in most of these latter sites is high, the better results of M8 confirm the absence of significant deviations of palaeodeclination from the expected value.

Palaeomagnetic results in the Internal Zone of the eastern Betics thus show a different pattern than the one found in older units elsewhere in the Betics. Rotated and unrotated areas can be recognized, with some rotations being of great magnitude. Counterclockwise rotations are found at left-lateral faults, although data are too scarce to define a general behaviour. The observed rotation pattern can be described as non-systematic. The age of block rotations is younger than Serravalian to early Tortonian (15–10 m.y.), which is the age of the oldest studied unit. Several sites of a late Tortonian to Messinian age are also rotated. Thus, a deformation due to recent movements of faults can be recognized. Rotations seem to be related to localized simple shearing of the upper crust within the compressive stress field due to the N140 convergence of Africa and the Iberian Peninsula since the late Tortonian (Vegas, 1992). In contrast, systematic rotations of the External Zones seem to be related to the detachment of the Mesozoic cover from the Hercynian basement.

Acknowledgements

We wish to thank L. Faynot, M. Perrin, M. Prévot and B. Smith (Université Montpellier II) for their help. We also wish to thank S. Allerton (Univ. Oxford) for a first correction of the manuscript, and two reviewers, E. Platzman and M. Westphal for their useful comments and suggestions. This work was carried out with the support of a FPU postdoctoral grant from the Spanish Ministry of Education and Science and projects PB92-0193 (DGICYT, Spain) and CI1-CT94-0114 (European Union). Publication No. 402, Dpto. de Física de la Tierra I, Universidad Complutense Madrid.

References

Allerton, S., Lonergan, L., Platt, J.P., Platzman, E.S. and McClelland, E., 1993. Palaeomagnetic rotations in the eastern Betic Cordillera, southern Spain. Earth Planet. Sci. Lett., 119: 225–241.

Allerton, S., Reicherter, K. and Platt, J.P., 1994. A structural and palaeomagnetic study of a section through the eastern Subbetic, Southern Spain. J. Geol. Soc. London, 151: 659–668.

Araña, V. and Vegas, R., 1974. Plate tectonics and volcanism in the Gibraltar Arc. Tectonophysics, 24: 197–212.

Bellon, H., Bau, N.Q., Chaumont, V. and Phillipet, J.C., 1981a. Implantation ionique de l'argon dans une cible support. Application au traçage isotopique de l'argon contenu dans les mineraux et les roches. C. R. Acad. Sci. Paris, pp. 977–980.

Bellon, H., Bizon, G., Calvo, J.P., Elizaga, E. Gaudant, J. and López Martínez, N., 1981b. Le volcan du Cerro del Monagrillo (Province de Murcia): âge radiométrique et corrélations avec les sédiments néogènes du bassin de Hellin (Espagne). C. R. Acad. Sci. Paris, 292: 1035–1038.

Bellon, H., Bordet, P. and Montenat, C., 1983. Chronologie du magmatisme néogène des Cordillères Bétiques (Espagne Meridionale). Bull. Soc. Geol. Fr., 25(2): 205–217.

Besse, J. and Courtillot, V., 1991. Revised and synthetic apparent polar wander paths of the African, Eurasian, North American and Indian plates, and true polar wander since 200 M.a. J. Geophys. Res., 96(B3): 4029–4050.

Bógalo, M.F., Osete, M.L., Ancochea, E. and Villalain, J.J., 1994. Estudio paleomagnético del volcanismo de Campos de Calatrava. Geogaceta, 15: 109–112.

Calvo, M., Osete, M.L. and Vegas, R., 1994. Palaeomagnetic rotations in opposite senses in southeastern Spain. Geophys. Res. Lett., 21(9): 761–764.

Cande, S.C. and Kent, D.V., 1995. Revised calibration of the geomagnetic polarity timescale for the Late Cretaceous and Cenozoic. J. Geophys. Res., 100(B4): 6093–6095.

Collinson, D.W., 1983. Methods in Rock Magnetism and Paleomagnetism. Techniques and Instrumentation. Chapman and Hall, London, 503 pp.

Comas, M.C., García-Dueñas, V. and Jurado, M.J., 1992. Neogene extensional tectonic evolution of the Alboran Basin from MCS data. Geo-Mar. Lett., 12: 157–164.

de Larouziere, F.D., Bolze, J., Bordet, P. Hernandez, J. Montenat, C. and Ott D'Estevou, P., 1988. The Betic segment of the lithospheric trans-Alborán shear zone during the late Miocene. Tectonophysics, 152: 41–52.

Demarest, H., 1983. Error analysis for the determination of tectonic rotation from paleomagnetic data. J. Geophys. Res., 88(85): 4321–4328.

Di Battistini, G., Toscani, L., Iacarino, S. and Villa, I.M., 1987. K/Ar ages and the geological setting of calc-alkaline volcanic rocks from Sierra de Gata, S.E. Spain. Neues Jahrb. Miner. Monatsh., H8: 369–383.

Feinberg, H., Saddiqi, O. and Michard, A., 1996. New constraints on the bending of the Gibraltar Arc from paleomagnetism of the Ronda peridotites (Betic Cordilleras, Spain). In: A. Morris and D.H. Tarling (Editors), Paleomagnetism and Tectonics of the Mediterranean Region. Geol. Soc. London, Spec. Publ., 105: 43–52.

Fisher, R.A., 1953. Dispersion on a sphere. Proc. R. Soc. London, A217: 295–305.

Kirschvink, J.L., 1980. The least-squares line and plane and the analysis of palaeomagnetic data. Geophys. J. R. Astron. Soc., 62: 699–718.

Levêque, F., 1992. Confrontation des données biochronologiques et magnétostratigraphiques dans les gisements continentaux du paléogène européen. Etalonnage temporel de l'echelle biochronologique mammalienne. Diplome de doctorat, Univ. Montpellier II, 249 pp.

López Ruiz, J. and Rodríguez Badiola, E., 1980. La región volcánica neógena del sureste de España. Est. Geol., 36: 5–63.

Lowrie, W. and Heller, F., 1982. Magnetic properties of marine limestones. Rev. Geophys. Space Phys., 20: 171–192.

Mazaud, A., Galbrun, B., Azema, J., Enay, R., Fourcade, E. and Rasplus, L., 1986. Données magnétostratigraphiques sur le Jurassique Supérieur et le Berriasien du NE des cordilliéres Bétiques. C. R. Acad. Sci. Paris, 302, Sér. II, 18: 1165–1170.

McFadden, P.L. and McElhinny, M.W., 1988. The combined analysis of remagnetization circles and direct observations in paleomagnetism. Earth Planet. Sci. Lett., 87: 161–172.

Montenat, C., D'Estevou, P.O.H. and Masse, P., 1987. Tectonic–sedimentary characters of the Betic–Neogene basins evolving in a crustal transcurrent shear zone (SE-Spain). Bull. Cent. Rech. Explor. Prod. ELF-Aquitaine, 11(1): 1–22.

Nobel, F.A., Andriessen, P.A.M., Hebera, E.H., Priem, H.N.A. and Rondecl, H.E., 1981. Isotopic dating of the post-alpine neogene volcanism in the Betic Cordilleras, Southern Spain. Geol. Mijnbouw, 60: 209–214.

Ogg, J.G., Steiner, M.B., Company, M. and Tavera, J.M., 1988. Magnetostratigraphy across the Berriasian–Valanginian stage boundary (Early Cretaceous) at Cehegín (Murcia province, southern Spain). Earth Planet. Sci. Lett., 87: 205–215.

Osete, M.L., Freeman, R. and Vegas, R., 1988. Preliminary palaeomagnetic results from the Subbetic Zone (Betic Cordillera, southern Spain): kinematic and structural implications. Phys. Earth Planet. Inter., 52: 283–300.

Osete, M.L., Freeman, R. and Vegas, R., 1989. Paleomagnetic evidence for block rotations and distributed deformation of the Iberian–African plate boundary. In: C. Kissel and C. Laj (Editors), Paleomagnetic Rotations and Continental Deformation. NATO ASI Series, Mathematical and Physical Sciences, 254. Kluwer Academic Publishers, Dordrecht, pp. 381–391.

Platzman, E., 1992. Paleomagnetic rotations and the kinematics of the Gibraltar arc. Geology, 20: 311–314.

Platzman, E. and Lowrie, W., 1992. Paleomagnetic evidence for rotation of the Iberian Peninsula and the External Betic Cordillera, Southern Spain. Earth Planet. Sci. Lett., 108: 45–60.

Vegas, R., 1992. Sobre el tipo de deformación distribuida en el contacto entre Africa y la Península Ibérica. In: M.L. Osete and M. Calvo (Editors), Física de la Tierra: Paleomagnetismo y Tectónica en las Cordilleras Béticas. Ed. de la Universidad Complutense, Vol. 4, pp. 41–56.

Villalaín, J.J., 1995. Estudio paleomagnético de la Béticas oc-

cidentales y sus implicaciones tectónicas. Descripción de una reimanación regional neógena. PhD Thesis, Universidad Complutense de Madrid, 225 pp.

Villalaín, J.J., Osete, M.L., Vegas, R., García-Dueñas, V. and Heller, F., 1994. Widespread Neogene remagnetization in Jurassic limestones of the South-Iberian paleomargin (Western Betics, Gibraltar Arc). Phys. Earth Planet. Inter., 85: 15–33.

Völk, H., 1966. Zur Geologie und Stratigraphie des Neogenbeckens von Vera, Südost-spanien. PhD Thesis, University of Amsterdam, 166 pp.